Pulsed NMR Study of ^1H and ^{19}F Spin–Lattice Relaxation and Cross Relaxation in Poly(vinylidene fluoride)

Bruce R. McGarvey*

Department of Chemistry, University of Windsor, Windsor, Ontario N9B 3P4, Canada

Shulamith Schlick

Department of Chemistry, University of Detroit, Detroit, Michigan 48221.
Received June 6, 1983

ABSTRACT: Spin–lattice relaxation times T_1 for ^1H and ^{19}F in the α(II) phase of poly(vinylidene fluoride) (PVDF) were measured in the temperature range 150–400 K. Regions of exponential and nonexponential decay of magnetization as a function of time were detected. Above 250 K two sets of T_1 values for each nucleus were deduced. The fast decay is identical in ^1H and ^{19}F experiments. The results are interpreted and simulated in terms of a model which includes homonuclear and heteronuclear dipolar interactions and a paramagnetic contribution to nuclear relaxation, which dominates at low temperatures, and assumes the presence of two phases with different relaxation characteristics. Results obtained in this study are compared with previous NMR studies and with recent ESR measurements of peroxy labels in α-PVDF.

I. Introduction

Poly(vinylidene fluoride) (PVDF) has attracted considerable interest recently because of its polarization properties in the β(I) phase. Many studies are focused on piezoelectric, pyroelectric, and ferroelectric properties of PVDF and its technological potential.[1-3] Attempts to calculate theoretically the pyroelectric coefficient were based on assuming changes of libration amplitude with temperature but quantitative agreement is rather poor.[4] Better agreement has been obtained recently by assuming a reversible temperature dependence of the degree of crystallinity.[5] In this model the crystallinity decreases as the temperature increases and only the crystalline portion contributes to polarization.

It has been amply demonstrated that line widths and relaxation time measurements of solid polymers by nuclear magnetic resonance (NMR) reveal details of the polymer motion and are sensitive to the presence of amorphous and crystalline phases.[6] Thus the NMR technique is well suited for study of the temperature-dependent motional processes in PVDF that might lead to a more detailed picture of the polarization effects. Most NMR studies were performed on the α(II) phase of PVDF which is the stable phase obtained when the polymer is synthesized. This phase, because of its crystalline structure, has no net polarization effects but study of its properties is useful for understanding the properties of the β(I) phase.

Previous NMR studies of PVDF include ^1H and ^{19}F line widths and second moments[7-9] and a report of ^1H line width for oriented PVDF films as a function of the angle between the magnetic field and the draw direction.[10] Pulsed NMR T_1, $T_{1\rho}$, and T_2 measurements of ^1H and ^{19}F at 30 MHz in α-PVDF have been reported by McBrierty, Douglass, and Weber.[11] In addition, the ^1H–^{19}F cross relaxation has been examined in detail by a study of the transient Overhauser effect in α-PVDF[12] and in blends of PVDF with poly(methyl methacrylate) (PMMA) and with poly(ethyl methacrylate) (PEMA).[13] A very recent NMR study of proton line width anisotropy in β-PVDF has also been published.[14]

Molecular motion in solid polymers can also be studied by using the peroxy radicals as probes.[15] Peroxy polymers are usually formed by high-energy irradiation in the presence of oxygen and can be studied by electron spin resonance (ESR). A specific motional model can be deduced by simulating the averaging of the g anisotropy as a function of temperature. Recent applications of this approach include studies of motion in poly(tetrafluoroethylene) (PTFE)[16] and in PVDF.[17] In PVDF ESR spectra have been interpreted by assuming a C–O bond rotation of the peroxy group –OO· with 180° jumps below 280 K and a helical twisting motion of the end of the polymer chain above 280 K. The fundamental question that arises in relation to these studies is to what extent ESR studies of the peroxy probe reflect the polymer environment, the intrinsic properties of the probe, or the deformation of the probe environment as a result of high-energy irradiation. This latter aspect is particularly relevant in view of a recent detection, by electron spin echo, of CH_3 displacement in lithium acetate dihydrate due to high-energy irradiation.[18]

We chose to clarify some of the questions concerned with ESR results as well as with previous NMR studies by measuring ^1H and ^{19}F spin–lattice relaxation times at 90.02 MHz for protons and 84.70 MHz for fluorine in the temperature range 150–400 K. The results obtained are examined and compared with previous studies.[11,12]

Experimental details are given in section II. Spin–lattice relaxation, T_1, data for ^1H and ^{19}F are described in section III. In section IV the experimental results are discussed in view of the theoretical predictions and in relation to the dynamics of the α-PVDF chain. Section V compares present results with various NMR studies. Section VI contains comparison of the present NMR study with peroxy-label ESR results.

II. Experimental Section

Solid PVDF is semicrystalline, with a crystallinity of ~50%.[2] For a melt-crystallized polymer, the α(II) phase is obtained, having a tgtg$^-$ conformation.[19,20] This is the form studied here and reported in ESR experiments.[17] The glass transition temperature for the polymer is ~240 K and the melting point is 445 K.

PVDF from Aldrich was used without further purification and was measured in evacuated 9-mm tubes.

NMR spectra were measured at 90.02 MHz for protons and 84.70 MHz for fluorine with a Bruker CXP-100 high-power FT spectrometer having a linear response over a bandwidth of ~1 MHz. Quadrature detection was used, with the spectrometer frequency at the center of spectrum. The 90° pulse time was less than 4 μs, corresponding to $B_1 \sim 17$ G. The dead time of the detection system was less than 3 μs.

The spectra measured at low temperatures had the typical flat-top line shapes corresponding to a static system of two interacting nuclei. As the temperature increased, a more Lorentzian line shape was observed. At 300 K the line widths, measured at half-maximum intensity, were ~20 kHz for ^1H and ~17 kHz for ^{19}F. The value of B_1 and the dead time of the spectrometer system

0024-9297/84/2217-2392$01.50/0

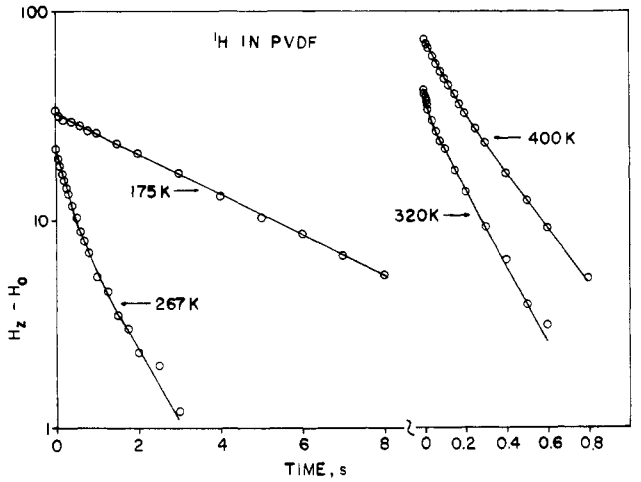

Figure 1. Decay of proton magnetization in T_1 measurements at 175, 267, 320, and 400 K. Solid lines are calculated from a three-parameter fit, eq 1, at 175 K and from a four-parameter fit, eq 2, at the other temperatures.

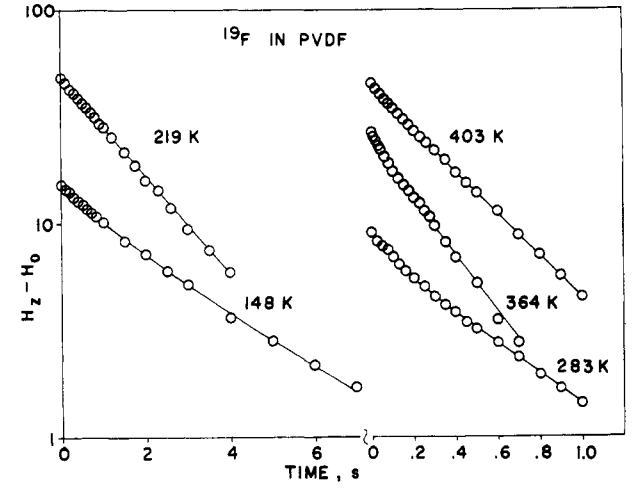

Figure 2. Decay of fluorine magnetization in T_1 measurements at 148, 219, 283, 364, and 403 K. Solid lines are calculated from a three-parameter fit at 219 K and from a four-parameter fit at the other temperatures.

are adequate for detection of the spectra, and therefore it was not deemed necessary to use the solid echo method.

T_1 measurements were performed by using a π–τ–$\pi/2$ pulse sequence. In some experiments, particularly at low temperatures and long values of T_1, a shorter than 90° or 180° pulse time was used, in order to reduce the waiting time between pulse sequences. The inverting pulse time was not shorter than 150° when this was done.

The temperature was controlled and measured by a Bruker BVT-1000 variable-temperature accessory. The temperature stability is within ±2 K.

III. Results

Decay of magnetization for a π–τ–$\pi/2$ pulse sequence at different temperatures for ^{1}H and ^{19}F are shown in Figures 1 and 2, respectively. Regions of exponential decays and also deviation from exponentiality are detected for both nuclei. For an exponential decay the value of T_1 was obtained by a three-parameter fit of $\langle H_z \rangle$:

$$\langle H_z \rangle = M - Ne^{-t/T_1} \quad (1)$$

The simulated parameters are M, N, and T_1, with M practically identical with the measured value of the equilibrium magnetization H_0. For magnetization decays deviating from exponentiality, the experimental results were simulated by using a four-parameter fit of $\langle H_z \rangle$:

$$\langle H_z \rangle = H_0 - W_f e^{-t/T_{1(\text{fast})}} - W_s e^{-t/T_{1(\text{slow})}} \quad (2)$$

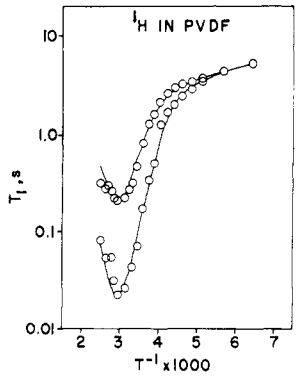

Figure 3. Spin–lattice relaxation times T_1 for protons in α-poly(vinylidene fluoride) at 90.02 MHz vs. reciprocal temperature.

This simulation implies that the total decay is a sum of two exponential decays. W_f, W_s, T_1(fast), and T_1(slow) are the fitted parameters and represent respectively the weight of the two decays and their decay constants. It is important to note that such a four-parameter fit is the simplest way to interpret deviation from exponentiality of the measured magnetization. At this point the only justification we present for this treatment of data is simplicity and also the fact that all data can be well simulated in this way. A good fit to experimental results does not necessarily imply a correct physical picture. However, cross relaxation usually leads to decays that are a sum of two exponentials[21] and ^{1}H–^{19}F cross relaxation has been detected in PVDF.[12] We will elaborate more on this subject in section IV. Implicit in this treatment of data is the fact that the accuracy of the preexponential parameters and of the decay constants is reduced as the intensity of one component of the decay decreases or if the decay constants are not very different.

We now discuss in more detail results for ^{1}H and ^{19}F.

1. T_1 of ^{1}H. Exponential decays are obtained between 155–200 K. Between 200–240 K deviations from exponentiality were observed, with T_1(fast) and T_1(slow) not very different. By comparing experimental decays with results of three- and four-parameter simulations, the following procedure was adopted: T_1(slow) was deduced from eq 2 and T_1(fast) was obtained by using eq 1. Above 240 K all decays were simulated by using eq 2. Results are summarized in Figure 3, where T_1(fast) and T_1(slow) are plotted as a function of inverse temperature. It is clear from Figure 3 that the two sets of T_1 values have a basic similarity; i.e., the minimum value of T_1 for each component is, within experimental error, at the same temperature, and the same T_1 value is observed for both components in the limit of low temperature.

2. T_1 of ^{19}F. Unlike ^{1}H results, decays of magnetization are not exponential in the low-temperature range, 148–190 K and become clearly exponential in the range 190–240 K. Similarly to ^{1}H results, all decays deviate from exponentiality above 250 K. Because of the more complex behavior of the magnetization for ^{19}F, we inspected and verified the data treatment method by plotting at several temperatures the difference between the observed value of the magnetization and the best fit to single- and double-exponential decays, as shown in Figure 4. At all temperatures shown, except at 213 K, the deviation obtained by assuming a single-exponential decay is typical of the case where the magnetization is a sum of two exponentials.[22] Also, the absolute deviations obtained by assuming a two-exponential decay are not larger than 1.3%, whereas the maximum deviation corresponding to a single-exponential fit is 5.6%. At 213 K, and in the entire range 190–240 K, both simulation methods give, as ex-

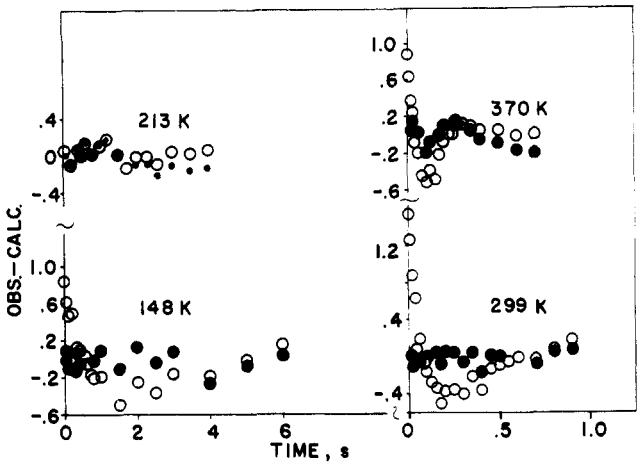

Figure 4. Deviation plot for single-exponential (○) and double-exponential (●) simulation of ^{19}F magnetization in T_1 experiments at indicated temperatures. Maximum reading for the magnetization is 16 at 213 K and 15 at the other temperatures. Some points were omitted, for clarity.

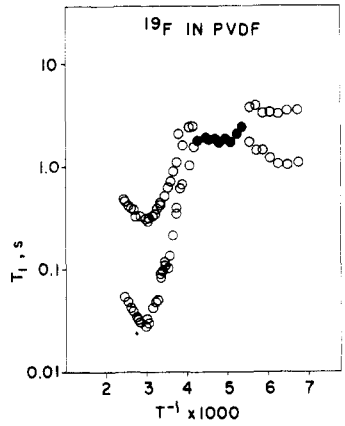

Figure 5. Spin–lattice relaxation times T_1 for ^{19}F in α-poly(vinylidene fluoride) at 84.70 MHz vs. reciprocal temperature. Filled circles (●) represent values obtained by single-exponential simulation; all other points are obtained by a double-exponential simulation.

pected for an exponential decay, small and similar deviations from measured values. The T_1 values thus obtained are plotted in Figure 5.

Inspection of Figure 2 shows that the decay at 364 K deviates slightly from a double-exponential behavior. This shape is typical of decays in the range 335–380 K and is also evident in Figure 4 for data at 370 K, where the plotted deviations do not follow the pattern of deviation observed at the other temperatures shown. This type of decay can be simulated by adding a small component with a negative preexponential factor and a decay coefficient slightly longer than T_1(slow) obtained for the data using eq 2. This effect has not been detected clearly in ^1H measurements and will be discussed later in section IV.

3. Intensity of the Fast Component. In both sets of measurements, for ^1H and ^{19}F, the intensity of the fast relaxing component decreases as the temperature increases. Results are plotted in Figure 6. The intensity of the fast component in ^1H measurements is larger than in ^{19}F measurements, the ratio in the vicinity of the minimum value of T_1 being ~60/40.

IV. Discussion

Above 250 K the decay curves of both ^1H and ^{19}F can be fitted to a two-exponential decay yielding two T_1 values. The two T_1 values, when plotted against temperature, yield

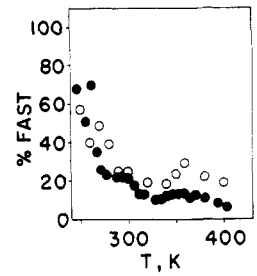

Figure 6. Percentage of the fast decaying component of magnetization for ^1H (○) and ^{19}F (●) as a function of temperature. Some points were omitted, for clarity.

curves that minimize at the same temperature. Furthermore, the shorter T_1 vs. temperature curves are identical, within experimental error, for both ^1H and ^{19}F. The longer T_1 curves are similar but not identical. Below 250 K, T_1 values for both nuclei reach a plateau. For ^1H a single-exponential decay is observed in this region while for ^{19}F a double-exponential decay is detected in the interval 150–200 K and a single decay in the interval 200–250 K. We will first focus our attention on the region above 250 K where a double-exponential decay was found for both nuclei.

Nonexponential decays in polymeric systems are not new and can be due to several possible sources. (1) Separate contributions from crystalline and amorphous phases[6] can give rise to a double-exponential decay. (2) Spin diffusion in multiphase polymeric systems has been shown[23] to lead to a double-exponential decay and a complex temperature dependence for the T_1 values. (3) It has been shown[24] that cross relaxation between ^1H and ^{19}F can lead to a double-exponential decay under certain circumstances and a double decay observed[25] for the low-temperature phase of *o*-carborane has been attributed to cross relaxation ^1H and ^{11}B.

The first two sources of nonexponential decay, mentioned above, will not predict a common fast decay term for both ^1H and ^{19}F in the system while the cross relaxation mechanism will predict it. The existence of a strong cross relaxation term in α-PVDF has already been demonstrated by measurement of the transient Overhauser effect (TOE)[12] in α-PVDF. Thus any attempt to explain our results must start with a theory that includes this effect.

Cross relaxation results from the dipolar interaction between ^1H and ^{19}F spins and has generally been treated by using the Solomon equations[24] which assume the nuclear relaxation can be expressed by the set of coupled equations.

$$(dH_z/dt) = -R_{HH}(H_z - H_0) - R_{HF}(F_z - F_0) \quad (3)$$

$$(dF_z/dt) = -R_{FF}(F_z - F_0) - R_{FH}(H_z - H_0) \quad (4)$$

where H_z, F_z, H_0, and F_0 are the z component of proton and fluorine magnetizations at time t and at thermal equilibrium, respectively, and

$$R_{ij} = (T_1)_{ij}^{-1} \quad (5)$$

These equations were originally proposed for liquid systems in which a common spin temperature could be assumed. McBrierty and Douglass[12] have shown that they should apply to the α-PVDF system we are studying, at least in the temperature regions above 250 K that we are discussing here.

Solution of (3) and (4) leads to

$$(H_z - H_0)/H_0 = A_H e^{D_+ t} + B_H e^{D_- t} \quad (6)$$

$$(F_z - F_0)/F_0 = B_H e^{D_+ t} + A_H e^{D_- t} \quad (7)$$

with

$$D_{\pm} = -(1/2)(R_{HH} + R_{FF}) \pm (1/2)[(R_{HH} - R_{FF})^2 + 4R_{HF}R_{FH}]^{1/2} \quad (8)$$

The coefficients A_H and B_H depend on the pulse sequence used for measuring T_1. For a π-τ-$\pi/2$ pulse sequence

$$A_H = 2(D_- + R_{HH})/(D_+ - D_-) \quad (9)$$

$$B_H = -2(D_+ + R_{HH})/(D_+ - D_-)$$

The ratio of A_H/B_H is, however, not dependent on the actual pulse sequence. We see in eq 6 and 7 that a double-exponential decay is expected when A_H and B_H are similar in magnitude and eq 8 and 9 reveal that this happens when $R_{HF}R_{FH}$ is similar in magnitude to $(R_{HH} - R_{FF})^2$.

Note that eq 6 and 7 both involve the same two relaxation terms: $T_1(\text{fast}) = -D_-^{-1}$ and $T_1(\text{slow}) = -D_+^{-1}$ (assuming that $R_{HH} > R_{FF}$). These equations predict that both ^{19}F and ^1H should have double-exponential decays involving the same fast and slow T_1's but would differ in the relative importance of the two decays. Thus cross relaxation can explain our observation of the same fast T_1 at all temperatures above 250 K but it cannot explain all our results because the slow T_1 of ^1H differs significantly from that observed for ^{19}F in the same temperature region.

Our results could be explained by postulating that the polymer consists of at least two phases, crystalline and amorphous, and that cross relaxation is important in both. In this case we would expect a four-exponential decay involving four T_1's. Spin diffusion between the phases would increase the complexity but would still lead to a four-exponential decay unless domain size were extremely small. It is not easy to detect such a decay and in general a multiexponential decay can be fitted quite nicely to a two-exponential decay. As mentioned earlier, we do have some data for ^{19}F as illustrated in Figure 4 that can be better fitted to a three-exponential decay than a two-exponential one. Our attempts to do fittings of a multiexponential decay to a two-exponential function have shown that T_1(fast) is generally close in value to the shortest T_1 in the multiexponential system and that T_1(slow) represents some sort of average of the other T_1's. Thus, it is expected, that in a two-phase system we would extract the same T_1(fast) for both ^1H and ^{19}F appropriate to one of the two phases and get somewhat different values for T_1(slow) because the average will not be the same for ^1H and ^{19}F due to the different values of A_H and B_H. If we are correct in this analysis, then any attempt to do a theoretical analysis of the results should concentrate on T_1(fast) vs. temperature curve which is common to both ^1H and ^{19}F.

If the main contribution to the R_{ij}'s is dipolar and we further assume that we can neglect intermolecular interactions, then the proton contribution to R_{HH} comes from the other proton on the $-CH_2-$ group and can be written[26] as

$$R_{HH}(\text{H-H}) = \frac{3\gamma_H^4\hbar^2}{10r_{HH}^6}\left[\frac{\tau_c}{1+\omega_H^2\tau_c^2} + \frac{4\tau_c}{1+4\omega_H^2\tau_c^2}\right] \quad (10)$$

where r_{HH} is the interproton distance.

The proton–fluorine contribution involves four fluorines on adjacent $-CF_2-$ groups and is obtained by assuming a two-spin H–F system and a common spin temperature. We obtain

$$R_{HH}(\text{H-F}) = \frac{2\gamma_H^2\gamma_F^2\hbar^2}{5r_{HF}^6}\left[\frac{6\tau_c}{1+(\omega_H+\omega_F)^2\tau_c^2} + \frac{\tau_c}{1+(\omega_H-\omega_F)^2\tau_c^2} + \frac{3\tau_c}{1+\omega_H^2\tau_c^2}\right] \quad (11)$$

$$R_{HF}(\text{H-F}) = \frac{2\gamma_H^2\gamma_F^2\hbar^2}{5r_{HF}^6}\left[\frac{6\tau_c}{1+(\omega_H+\omega_F)^2\tau_c^2} - \frac{\tau_c}{1+(\omega_H-\omega_F)^2\tau_c^2}\right] \quad (12)$$

r_{HF} is the average proton–fluorine distance, and

$$\tau_c = \tau_0 e^{E_a/RT} \quad (13)$$

The relaxation rates R_{FF} and R_{FH} are obtained by changing appropriate labels in eq 10–12.

From the crystal structure of α-PVDF[19,20,27] $r_{HH} \sim 1.75$ Å, $r_{HF} \sim 2.42$ Å, and $r_{FF} \sim 2.6$ Å. The relaxation rates can now be estimated for α-PVDF, making the key assumption that the relaxation of the system can be described by a single correlation time τ_c. By making this assumption we imply not only that all chain segments have the same τ_c but, in addition, that the different dipolar contributions to relaxation, such as proton–proton, proton–fluorine, and fluorine–fluorine have the same correlation time.

The only other mechanism that could make a contribution to the R_{ij}'s is the anisotropy of the chemical shift in ^{19}F and this will only affect the value of R_{FF}. The contribution to T_1 from a large anisotropy in the chemical shift is given by the equation[28]

$$T_1^{-1} = (2/15)(\sigma_\parallel - \sigma_\perp)^2\omega_F^2\tau_c/(1+\omega_F^2\tau_c^2) \quad (14)$$

If we take $(\sigma_\parallel - \sigma_\perp) = 120$ ppm[26] and $r_{FF} = 2.6$ Å, the ratio of eq 14 to R_{FF}(F–F) from the dipolar interaction varies from 0.25 when $\tau_c \ll \omega_F^{-1}$ to 0.63 when $\tau_c \gg \omega_F^{-1}$. When we include the R_{FF}(F–H) contribution to R_{FF}, however, the ratio of eq 14 to the total R_{FF} drops to 0.044 when $\tau_c \ll \omega_F^{-1}$ and to 0.013 when $\tau_c \gg \omega_F^{-1}$. Thus we can safely ignore the chemical shift anisotropy in our analysis.

Equations 10–12 can be rewritten as

$$R_{HH} = Af_A(\tau_c) + Bf_B(\tau_c)$$
$$R_{HF} = Bf_C(\tau_c) \quad (15)$$
$$R_{FF} = Cf_D(\tau_c) + Bf_E(\tau_c)$$

with

$$A = \frac{3\gamma_H^4\hbar^2}{10r_{HH}^6}$$
$$B = \frac{2\gamma_H^2\gamma_F^2\hbar^2}{5r_{HF}^6} \quad (16)$$
$$C = \frac{3\gamma_F^4\hbar^2}{10r_{FF}^6}$$

f_A, f_B, f_C, f_D, and f_E can be found by comparing eq 15 and 16 with eq 10–12. These equations allow us to discuss the shape of the temperature dependence of T_1(fast) as a function of the ratio of B and C to A. For the H–H, H–F, and F–F distances given above $(C/A) = 0.112$ and $(B/A) = 0.169$.

A plot of T_1(fast) vs. log $(\omega_H\tau_c)$ is equivalent to plotting T_1(fast) vs. T^{-1}. We have found that the shape of T_1(fast) vs. log $(\omega_H\tau_c)$ is little influenced by the ratio of (C/A) but

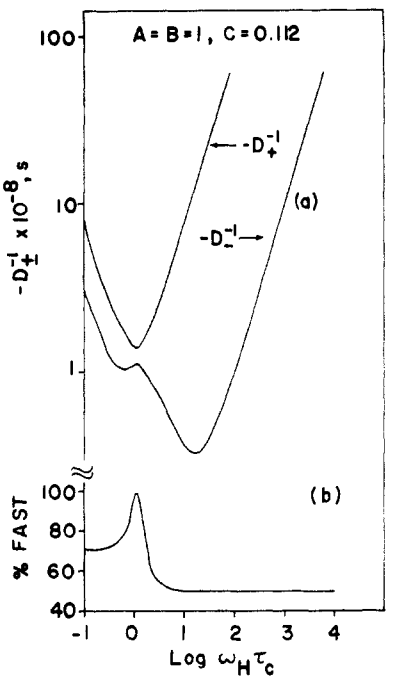

Figure 7. (a) Calculated values of $-D_+^{-1}$ and $-D_-^{-1}$ (eq 6–8) as a function of $\omega_H\tau_c$. (b) Calculated weight percentage of the fast decaying component of the magnetization ($100B_H/(A_H + B_H)$ in eq 6) as a function of $\omega_H\tau_c$. In (a) and (b), $A = B = 1$ and $C = 0.112$.

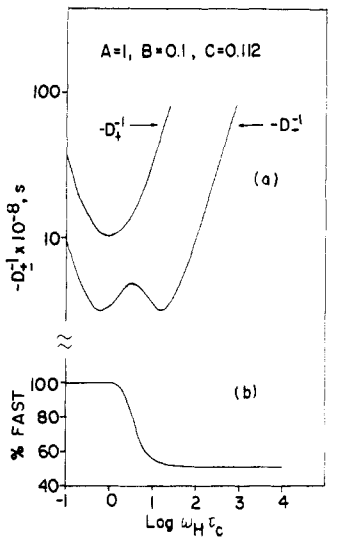

Figure 8. (a) Calculated values of $-D_+^{-1}$ and $-D_-^{-1}$ (eq 6–8) as a function of $\omega_H\tau_c$. (b) Calculated weight percentage of the fast decaying component of the magnetization ($100B_H/(A_H + B_H)$ in eq 6) as a function of $\omega_H\tau_c$. In (a) and (b), $A = 1$, $B = 0.1$, and $C = 0.112$.

is strongly dependent on (B/A). Plots of T_1(fast) and T_1(slow) for $(B/A) = 0$, 0.01, 0.1, and 1.0 are given in Figures 7–9, assuming $A = 1.0$. Also plotted is the percentage of fast decay for ^{1}H, which is $[100B_H/(A_H + B_H)]$. Examination of these theoretical plots reveals that for reasonable values of (B/A), T_1(fast) for ^{1}H should show a double minimum and should exhibit a two-exponential decay at low temperatures below and including the low-temperature minumum. A simple exponential decay would occur in the region of the high-temperature minimum. For ^{19}F the T_1(fast) would be detected only in the low-temperature interval including the low-temperature minimum where a double-exponential decay is obtained.

The low-temperature minimum comes from the dominance of the $(\omega_H - \omega_F)$ term in $f_B(\tau_c)$ at low temperatures.

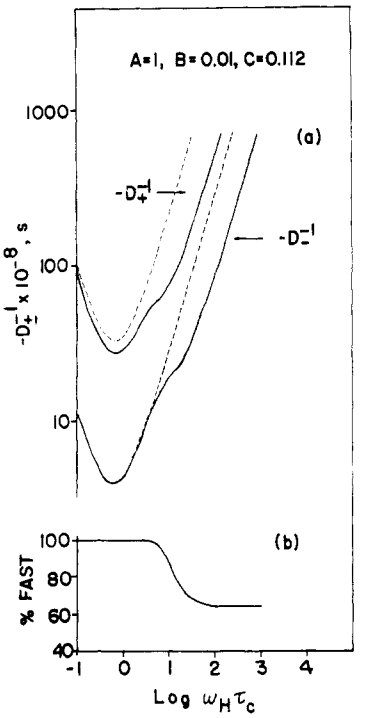

Figure 9. (a) Calculated values of $-D_+^{-1}$ and $-D_-^{-1}$ (eq 6–8) as a function of $\omega_H\tau_c$. (b) Calculated weight percentage of the fast decaying component of the magnetization ($100\,B_H/(A_H + B_H)$ in eq 6) as a function of $\omega_H\tau_c$. In (a) and (b), $A = 1$, $B = 0.01$, and $C = 0.112$. The broken lines have been calculated for $B = 0$, for comparison.

At very low temperatures $R_{HH} \rightarrow -R_{HF}$ and this accounts for the fact that $B_H \rightarrow A_H$ for high values of $\omega_H\tau_c$. In order to explain our results, we must assume that the minimum we see is the low-temperature one at $\omega_H\tau_c \approx 16$. Using the H–H, H–F, and F–F distances given above, we calculate from our equations that the low-temperature minimum would occur at T_1(fast) = 13 ms which is not too far from the experimental value of 24 ± 4 ms. Inclusion of intermolecular interactions and/or a small adjustment in the (B/A) ratio will bring the two numbers into exact agreement.

Before we try to fit theory and experiment over the whole temperature range, we must consider the results below 250 K which suggest an additional relaxation mechanism is important. The plateau observed at low temperatures is best accounted for by proposing the existence of paramagnetic impurities such as free radicals from the polymerization process or paramagnetic ions. Such a mechanism has been invoked before in cases where a T_1 plateau has been observed.[25] The paramagnetic relaxation rate is introduced in the form

$$R_p = R_0 e^{-E_p/RT} \tag{17}$$

and R_p can be directly added to R_{HH} and R_{FF}. Inspection of ^{1}H results, Figure 3, in the low-temperature region suggests trial values $E_p = 2.4$ kJ mol^{-1} and $R_0 = 1.2$ s^{-1}. The fact that the T_1(fast) plateau is smaller for ^{19}F than ^{1}H suggests that R_0 is larger for ^{19}F. This is not surprising and suggests that, on the average, the paramagnetic impurities are found closer to fluorine nuclei than protons in the polymer.

We have combined eq 17 with eq 15 and attempted to fit the theoretical equation to our experimental T_1(fast) vs. temperature curves. In doing so, we have chosen to assume the values of $(B/A) = 0.169$ and $(C/A) = 0.112$ which are predicted by the nuclear distances given above. We then adjusted the parameters A, E_a, E_p, τ_0, $(R_0)_H$, and

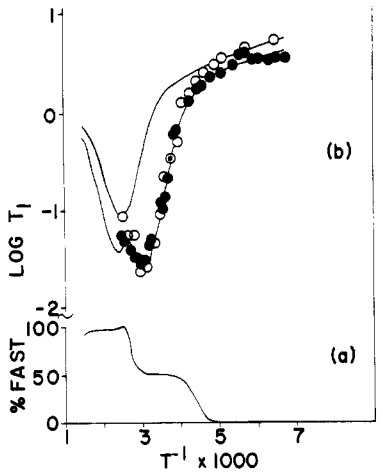

Figure 10. (a) Calculated percentage of the fast decaying component of magnetization ($100B_H/(A_H + B_H)$ in eq 6) as a function of inverse temperature. (b) Calculated values of log (T_1(fast)) as a function of inverse temperature. Experimental results for the fast decay of ^1H (○) and of ^{19}F (●) are indicated. Some experimental points are omitted, for clarity. (c) The parameters used for calculation are $A = 7.5 \times 10^9$ s^{-2}, $B = 0.169A$, $C = 0.112A$, $E_a = 39$ kJ/mol, $\tau_0 = 1.8 \times 10^{-14}$ s, $E_p = 2.4$ kJ/mol, $(R_0)_H = 1.25$ s^{-1}, $(R_0)_F/(R_0)_H = 1.3$, and τ_c(H–H)/τ_c(H–F) = 1.0.

$(R_0)_F$ to get a reasonable fit between experiment and theory. This is not too difficult as reasonable first approximations to E_p, $(R_0)_H$, and $(R_0)_F$ are obtained from the experimental curves below 250 K while A and τ_c at the minimum can be obtained from the experimental minimum itself. A simple fitting of the curve to some point between 250 K and the minimum serves to give a good estimate of τ_c at that temperature, from which τ_c and E_a can be estimated. Adjustments of these starting values gave a good fit for the following parameters: $A = 7.5 \times 10^9$ s^{-2}, $E_a = 39$ kJ mol^{-1}, $E_p = 2.4$ kJ mol^{-1}, $\tau_0 = 1.8 \times 10^{-14}$ s, $(R_0)_H = 1.25$ s^{-1}, and $(R_0)_F = 3.75$ s^{-1}. The calculated curve and experimental points are shown in Figure 10.

In many ways, the agreement between experiment and theory is reasonable. It is not completely satisfactory, however, in three things. (1) Experimentally, we should see indications of the higher temperature minimum in the ^1H data at the highest temperatures and none is found. (2) The percentage of fast component is 50% at the minimum and unless the second phase has much different parameters, this would mean that T_1(slow) would be identical for both ^1H and ^{19}F. (3) The T_1(slow) from theory minimizes at a much higher temperature than T_1(fast). Since our T_1(slow) is postulated in our model to be an average of T_1(fast) from one phase and T_1(slow) from two phases, it is difficult to account for the fact that our T_1(slow) minimizes at the same temperature as that of T_1(fast).

Our theoretical model is, of course, simplistic and it is of interest to consider what sort of alterations would tend to remove the three difficulties discussed above. We have used a simple two-phase model in our discussion and a multiphase model would of course be more realistic. It is difficult for the authors, however, to see how a multiphase model would remove any of the difficulties. We have assumed (as have many other investigators) that we can treat a given phase as having a unique correlation time τ_c. More likely we have a statistical distribution of τ_c's throughout a given phase. The main effect of most statistical distributions is to make each minimum broader and shallower and in the end will not produce a better fit or remove the above difficulties without introducing new ones at the same time. A more serious assumption in our equations (which were derived for liquid systems) is the assumption of a random rotational model in which a common τ_c can be used for all motions of the nuclei.

It is more likely that the motion is restricted, rather than random, and that some dipolar interactions are more affected than others by this motion. For example, if we assume that the most prominent motion is rotation about the polymer chain and that $-CH_2-CF_2-$ fragments rotate more or less as a unit, then r_{HH} and r_{FF} vectors would change their orientation relative to the magnetic field and their motion would make a significant contribution to R_{HH} and R_{FF}. The r_{HF} vector would, however, not change its orientation relative to the magnetic field and would make little contribution to the relaxation parameters controlling T_1. One could still use our present equations in this case by assuming the R_{ij}(H–H) and R_{ij}(F–F) terms have one correlation time while the R_{ij}(H–F) terms have a different and longer correlation time. Other motional models might take three different τ_c's: one for H–H terms, one for F–F terms, and one for H–F terms.

The two-τ_c model outlined above can resolve much of the difficulties seen in Figure 10. The high-temperature minimum comes from H–H, H–F, and F–F interactions while the low-temperature minimum comes only from H–F interactions. If we make τ_c for H–H and F–F interactions shorter than that for H–F interactions, the high-temperature minimum will broaden, become shallower, and move toward the low-temperature minimum. To illustrate this, we have arbitrarily taken τ_c(H–H) = τ_c(F–F) = 0.1τ_c(H–F) and then just adjusted the value of A from our previous fitted parameters to fit the theoretical curve to the experimental points. The calculated curve and experimental data are given in Figure 11. The new A value is 6.6×10^9 s^{-2} which is quite close to the theoretical value of 5.9×10^9 s^{-2} calculated from eq 16. It can be seen that the fit is greatly improved and many of the difficulties referred to above have disappeared.

The better fit obtained with the two-correlation time model is not proof of the validity of the model. However, the model is not an unreasonable one for α-PVDF, and the data certainly do not contradict such a model.

V. Comparison with Previous Studies of PVDF[11,12,19]

The major difference between T_1 values obtained in this study and those published[11] is that we observed, over most of the temperature range covered, nonexponential decays of magnetization for each nucleus, whereas exponential decays were reported previously. There are two possible reasons for this difference.

First, T_1 values previously measured[11] in the low-temperature range are shorter than those reported in this study, implying a larger paramagnetic term. We estimate $R_0 \sim 5.1$ s^{-1} and $E_p \sim 3$ kJ/mol in ref 11, compared with 1.25 s^{-1} and 2.4 kJ/mol respectively found in this study. We calculated the decay rates for this larger paramagnetic term and the other parameters as in Figure 11, and two effects are observed. As expected, lower T_1 values are obtained in the low-temperature limit. Also important for this discussion is the effect on the T_1 values for the slow decay. The minimum is lowered from 107 ms in Figure 11 to 87 ms; in other words, the two decays become *closer*. The relaxation times for the second phase are obviously lowered as well, and the result is that all decays are bunched closer together, making it harder to detect individual decays.

Second, a possibility exists that less scatter and a better signal-to-noise ratio is obtained in experiments at 90 MHz than at 30 MHz. Even small effects might make a dif-

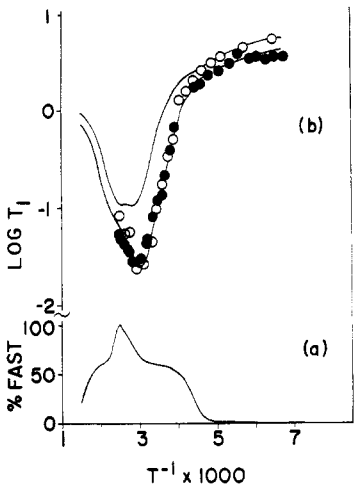

Figure 11. (a) Calculated percentage of the fast decaying component of magnetization ($100B_H/(A_H + B_H)$ in eq 6) as a function of inverse temperature. (b) Calculated values of log (T_1(fast)) as a function of inverse temperature. Experimental results for the fast decay of ^{1}H (○) and of ^{19}F (●) are indicated. Some experimental points are omitted, for clarity. (c) The parameters used for calculation are $A = 6.6 \times 10^9$ s^{-2}, $B = 0.169A$, $C = 0.112A$, $E_a = 39$ kJ/mol, $\tau_0 = 1.8 \times 10^{-14}$ s, $E_p = 2.4$ kJ/mol, $(R_0)_H = 1.25$ s^{-1}, $(R_0)_F/(R_0)_H = 1.3$, and τ_c(H–H)/τ_c(H–F) = 0.1.

ference, especially at temperatures where the two decay constants are not very far apart.

If we assume the single T_1's observed[11] are some sort of average of the two T_1's we measured, the results of their measurements and ours are in agreement. If we take our fitted value of $E_a = 39$ kJ mol^{-1}, we would predict the minimum we observed at 337 ± 4 K at 90 MHz would shift to 313 K at 30 MHz which agrees with the temperature found for the minimum. Since we found $(T_1)_{min}$ for the slow decay to be higher for ^{19}F than ^{1}H we would expect the average value at the minimum to be higher for ^{19}F, again in agreement with the published results.[11]

We conclude that in our experiments a lower paramagnetic term and possibly a better signal-to-noise ratio enabled us to extract more details of the relaxation process in PVDF.

VI. Comparison with Peroxy Probe Studies of Motion

ESR studies[17] suggest two types of motion in α-PVDF: a local CO bond rotation of the peroxy OO· group below 280 K and a helical twisting of the polymer chain which becomes detectable at ~250 K and is predominant above 280 K. ESR spectra at 298 K are well simulated by assuming a correlation time of 1×10^{-8} s for the helical twist motion and a correlation time shorter than 1×10^{-9} s for the CO bond rotation. NMR results obtained in this study can be explained by assuming one type of motion only. The correlation time at 298 K calculated from the "best" parameters used in this NMR study ($\tau_0 = 1.8 \times 10^{-4}$ s and $E_a = 39$ kJ mol^{-1}) is 1×10^{-7} s. This value is reasonably close to the value obtained for the chain motion in ESR studies and can therefore be identified with the same motion. This conclusion is strengthened by the fact that good agreement of theory with experimental NMR results is obtained only if the correlation time for H–H interaction is assumed to be shorter than for H–F interaction. This assumption is reasonable for a chain motion in which the H–F vector direction remains fixed relative to the magnetic field during the motion while the H–H vector direction is a function of time, as suggested in the ESR experiments. Further support to such a model is obtained in measurements of polarization as a function of time which suggest a concerted motion of eight monomeric units around the chain axis.[29]

It is possible that the absence of the local bond rotation in NMR experiments indicates that this motion is typical of the peroxy spin probe and not of the neat polymer.

NMR studies detect the presence of two phases in α-PVDF, crystalline and amorphous, while no such evidence is suggested in ESR studies. This fact might be related to mounting evidence for decrease of crystallinity[30] and profound changes in morphology of polymers on high-energy irradiation.[31] In view of this evidence it becomes logical to conclude that peroxy probe studies of polymers probably reflect the properties of the amorphous phase.

VII. Conclusion

Presence of amorphous and crystalline phases and proton–fluorine cross relaxation adds complexity to the NMR study of PVDF. All salient features of the spin–lattice relaxation results can be explained, however, by considering homonuclear and heteronuclear dipolar interactions with different correlation times as well as a paramagnetic contribution to relaxation.

Acknowledgment. We thank the referees for bringing to our attention two very important references. This work was supported by a grant from the National Science and Engineering Research Council of Canada.

References and Notes

(1) Hayakawa, R.; Wada, Y. *Rep. Prog. Polym. Phys. Jpn.* **1976**, *19*, 321.
(2) Kepler, R. G.; Anderson, R. A. *CRC Crit. Rev. Solid State Mater. Sci.* **1980**, *9*, 399.
(3) Broadhurst, M. G.; Davis, G. T. *Top. Appl. Phys.* **1979**, *33*, 285.
(4) Mopsik, J. J.; Broadhurst, M. G. *J. Appl. Phys.* **1975**, *46*, 4204.
(5) Kepler, R. G.; Anderson, R. A. *J. Appl. Phys.* **1978**, *49*, 4918. Kepler, R. G.; Anderson, R. A.; Lagasse, R. R. *Phys. Rev. Lett.* **1982**, *48*, 1274.
(6) McBrierty, V. J.; Douglass, D. C. *Phys. Rep.* **1980**, *63*, 61; *Macromol. Rev.* **1981**, *16*, 295.
(7) Slichter, W. P. *J. Polym. Sci.* **1957**, *24*, 173.
(8) Sasabe, H.; Saito, S.; Asahina, M.; Kakutani, H. *J. Polym. Sci., Part A-2* **1969**, *7*, 1405.
(9) Kakutani, H. *J. Polym. Sci., Part A-2* **1970**, *8*, 1177.
(10) Lando, J. B.; Olf, H. G.; Peterlin, A. *J. Polym. Sci., Part A-1* **1966**, *4*, 941.
(11) McBrierty, V. J.; Douglass, D. C.; Weber, T. A. *J. Polym. Sci., Polym. Phys. Ed.* **1976**, *14*, 1271.
(12) McBrierty, V. J.; Douglass, D. C. *Macromolecules* **1977**, *10*, 855.
(13) Douglass, D. C.; McBrierty, V. J. *Macromolecules* **1978**, *11*, 766.
(14) Douglass, D. C.; McBrierty, V. J.; Wang, T. T. *J. Chem. Phys.* **1982**, *77*, 5826.
(15) Schlick, S.; Kevan, L. *J. Am. Chem. Soc.* **1980**, *102*, 4622.
(16) Suryanarayana, D.; Kevan, L.; Schlick, S. *J. Am. Chem. Soc.* **1982**, *104*, 668. Schlick, S.; McGarvey, B. R. *J. Phys. Chem.* **1983**, *87*, 352.
(17) Suryanarayana, D.; Kevan, L. *J. Am. Chem. Soc.* **1982**, *104*, 6251.
(18) Narayana, M.; Kevan, L.; Schlick, S. *J. Phys. Chem.* **1982**, *86*, 196.
(19) Hasegawa, R.; Takahashi, Y.; Chatani, Y.; Tadokoro, H. *Polym. J.* **1972**, *3*, 600.
(20) Doll, W. W.; Lando, J. B. *J. Macromol. Sci., Phys.* **1970**, *B4*, 309. Bachman, M. A.; Lando, J. B. *Macromolecules* **1981**, *14*, 40.
(21) Standley, K. J.; Vaughan, R. A. "Electron Spin Relaxation Phenomena in Solids"; Adam Hilger Ltd.: London, 1969; Chapters 3 and 7.
(22) Kalantar, A. H. *J. Lumin.* **1982**, *27*, 13.
(23) Douglass, D. C.; McBrierty, V. J. *J. Chem. Phys.* **1971**, *54*, 4085.
(24) Solomon, I. *Phys. Rev.* **1955**, *99*, 559. Solomon, I.; Bloembergen, N. *J. Chem. Phys.* **1956**, *25*, 261.
(25) Reynhardt, E. C.; Watton, A.; Petch, H. E. *J. Magn. Reson.* **1982**, *46*, 453.
(26) Carrington, A.; McLachlan, A. D. "Introduction to Magnetic Resonance"; Harper & Row: New York, 1967; Chapter 11.

(27) It is interesting to note that in phase II (α) of PVDF the closest H–F distances are not all to the fluorine atoms on adjacent carbon atoms. The shortest H–F distances of H1, for instance, are to F2 and F3, on adjacent *different* carbon atoms and to F1′ and F2′ on carbons three bonds removed from the carbon to which H1 is connected (see ref 20).
(28) McConnell, H. M.; Holm, C. H. *J. Chem. Phys.* **1956**, *25*, 1289.
(29) Broadhurst, M. G., private communication.
(30) Yoda, O.; Kuriyama, I.; Odajima, A. *J. Mater. Sci. Lett.* **1982**, *1*, 451.
(31) Fujimura, T.; Hayakawa, N.; Kuriyama, I. *J. Appl. Polym. Sci.* **1982**, *27*, 4093.

Aromatic Ring Flips in a Semicrystalline Polymer

Ashok L. Cholli, Joseph J. Dumais, Alan K. Engel,† and Lynn W. Jelinski*
AT&T Bell Laboratories, Murray Hill, New Jersey 07974. *Received February 23, 1984*

ABSTRACT: We report a detailed analysis of the phenyl ring motions that occur in the semicrystalline polymer [aromatic-d_4]poly(butylene terephthalate). Solid-state deuterium NMR results show that there are three distinct motional regimes, consisting of (1) the crystalline regions, where the phenyl rings are static, (2) a region of intermediate mobility, in which the aromatic groups undergo slow 180° ring flips, and (3) the amorphous part, in which the rings undergo 180° flips ($\tau_c = 1.8 \times 10^{-6}$ s at 70 °C) superimposed on rapid, low-angle librational motions. The 180° ring flip process has an activation energy of 5.9 kcal/mol. The amount of each phase is in accord with density measurements. Whether a phenyl ring does or does not undergo a 180° ring flip is attributed to the conformational space surrounding that site. The phenyl ring flip process appears to be universal, occurring here as well as in small organic molecules, other synthetic polymers, and biopolymers. It can be used as a sensitive reporter of morphology in these materials. Pulse sequences are described for the selective observation of separate motional regions in polymers.

A dispersion in the rates of aromatic ring flips has been demonstrated elegantly by Wüthrich and co-workers,[1] who observed by solution-state proton NMR spectroscopy that the aromatic rings in bovine pancreatic trypsin inhibitor have different ring flip rates. These differences in phenyl ring flip rates were originally attributed to biological activity. However, the discovery of aromatic ring flips in the crystalline amino acid phenylalanine[2] suggested that the occurrence of these phenyl motions is not related to biological activity but reflects instead the local structure of the material. Phenyl ring flips have since been observed in several other solid polymers and biopolymers, including the crystalline peptide enkephalin,[3] the amorphous polymer polycarbonate,[4,5] epoxy resins,[6] polystyrene,[5,7] and drawn poly(ethylene terephthalate).[8]

Although phenyl ring flips have now been observed in a number of systems, several fundamental questions concerning aromatic ring flips remain unanswered, particularly in the area of semicrystalline polymers. Among these are the following: (1) Is a pure 180° flip model adequate to explain the motion of phenyl rings in polymers? (2) Do phenyl ring flips occur only in the amorphous regions of semicrystalline polymers? (3) What is the activation energy for a 180° ring flip in a semicrystalline polymer? (4) Is there a homogeneous (narrow) or heterogeneous (broad) distribution of phenyl ring flip rates in these systems?

We report here data bearing on these questions. This work involves a detailed solid-state deuterium NMR study of phenyl ring flips in poly(butylene terephthalate):[9]

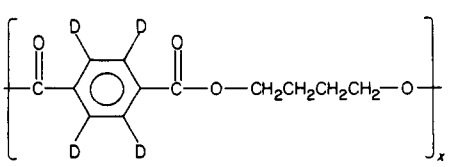

A phenyl ring flip in this system requires rotation about sp^2–sp^2 bonds. The aromatic and carbonyl groups participate in π-bond conjugation, causing the carbonyl–aromatic bonds to have partial double-bond character. The carbonyl groups and the intervening aromatic ring therefore tend to be coplanar. This aromatic system is predicted to have two predominant conformations, interconvertable by 180° flips.[10]

Deuterium NMR spectroscopy in the solid state is well suited for determining the details of local molecular motions in polymers.[5,11] The deuterium NMR spectrum of a static C–D bond (i.e., one that is not undergoing motion on the deuterium NMR time scale and has a correlation time $\tau_c > 10^{-3}$ s) consists of a Pake doublet that has a quadrupole splitting, $\Delta\nu_q$, of 128 kHz ($\Delta\nu_q$ is three-quarters of the quadrupole coupling constant, or $3e^2Qq/4h$). The electric field gradient tensor is axially symmetric, which means that there is a one-to-one correspondence between the orientation of the C–D bond with respect to the magnetic field and the frequency at which this orientation resonates. Furthermore, the symmetry axis of the field gradient tensor is along the C–D bond axis. Because the field gradient tensor is axially symmetric and since the molecular orientation of the principal axes of the field gradient tensor is known, the interpretation of deuterium line shapes in the presence of motion becomes straightforward.[5,11] In addition to depending on the jump angle for motion, deuterium NMR line shapes are also sensitive to the correlation time for motion when the correlation time is in the intermediate exchange regime (10^{-8} s $< \tau_c < 10^{-4}$ s).[11] Therefore, temperature-dependent solid-state deuterium NMR spectra can be used to extract information concerning both the *rate* and *angular range* of local polymer motions. Finally, measurements of spin–lattice relaxation times can also be used to verify the correlation times determined from the line shape analyses and can also be used to determine correlation times when the line shape is no longer sensitive to increased motional rates ($\tau_c < 10^{-8}$ s).[12]

Explicit examples of the deuterium NMR line shapes that are predicted for the deuterated aromatic ring of poly(butylene terephthalate) are shown in Figure 1. If the aromatic rings are static on the deuterium NMR time

† E. I. du Pont de Nemours and Co., Wilmington, DE 19898; current address: Sophia University, Tokyo 102, Japan.

0024-9297/84/2217-2399$01.50/0